

BIOCHEMICAL DIVERSITY AND COMPOSITION OF THE UNSTUDIED PATAGONIAN ENDEMIC PLANT *Benthamiella azurella* (skotts.) Soriano: ANTIOXIDANT, ANTIBACTERIAL AND CYTOTOXIC ACTIVITY ON VARIOUS HUMAN CELL LINES

DAFNE DÍAZ-HERNÁNDEZ¹, BORJA MARTINEZ-ALBARDONEDO¹, SALVADOR ARIJO², VÍCTOR SANHUEZA¹, JOSÉ BECERRA⁴, ROBERTO T. ABDALA-DÍAZ⁵ AND VÍCTOR FAJARDO¹

¹Laboratory of Natural Products, Department of Sciences, Faculty of Sciences, Magallanes University, Punta Arenas, Chile.

²Andalusian Institute of Blue Biotechnology and Development (IBYDA), Microbiology Department, Faculty of Sciences, Malaga University, Campus Universitario de Teatinos s/n, 29071 Malaga, Spain.

⁴Department of Botany, Faculty of Natural and Oceanographic Sciences, University of Concepcion, Concepción, Chile.

⁵Department of Ecology and Geology, Faculty of Science, Andalusian Institute of Blue Biotechnology and Development (IBYDA), Malaga University, Campus Universitario de Teatinos s/n, 29071 Malaga, Spain.

ABSTRACT

Benthamiella (Solanaceae) is an unstudied endemic genus of the Chilean-Argentinean Patagonia that thrives in harsh climatic and geographic conditions. This study provides a biochemical description of the aerial parts, roots, and polysaccharides of *B. azurella*, and evaluates their antioxidant, antiproliferative and antibacterial activity. GC-MS analysis of *B. azurella* roots polysaccharides identified significant amounts of arabinose, glucose and galacturonic acid. The FT-IR spectrum revealed a diverse range of functional groups. Both analyses suggest a complex polysaccharide structure that may enhance the sample's functional properties. Elemental analysis showed low nitrogen and sulfur content, while proximate analysis showed significant differences in carbohydrates, lipids, fiber, and ash content between the plant parts. Polyphenols quantification determined a higher concentration in the roots (6.66 ± 0.62 mg GAE g⁻¹ DW) compared to the aerial parts. Likewise, the highest antioxidant capacity was observed in the roots using the DPPH (89.43 ± 0.74 μ mol AAE g⁻¹ DW at 1818 μ g mL⁻¹) method. The aqueous root extract exhibited higher activity against colon cancer HCT-116 followed by aerial parts. Polysaccharides showed slight activity against hepatocytes cancer HepG2. The extracts behaved variably on the healthy keratinocytes HACAT cell line, tending to promote cell proliferation. Both, aqueous and ethanolic *B. azurella* solutions were non-toxic, did not show quorum quenching and antibacterial activity against human and fish bacterial strains at the tested concentrations. Finally, 21 metabolites, principally hydroxycoumarins, saponins and steroids derivatives were tentatively identified in the most active extract using LC-MS analysis. Further assays of *B. azurella* roots with cancer and healthy cell lines and new bacterial analysis at higher concentrations are recommended.

Keywords: *Benthamiella*, Patagonia, antioxidant, antibacterial, cytotoxicity, polysaccharides, LC-MS, metabolites profiles

1. INTRODUCTION

Patagonia, located in the extreme south of Chile and Argentina, is an underexplored area rich in unique natural resources. Its distinct geomorphology, climate, flora, and fauna, along with the traditional resources of its cultures, make it a valuable subject for multidisciplinary research [1]. Studies on Patagonia plants have identified extracts and metabolites with various biological activities, including antioxidant [2], cardiovascular [3], antimicrobial [4], insecticidal [5] and antiproliferative [6] properties. In Despite these findings, many native and endemic plants as the *Benthamiella* genus, remain unstudied.

The *Benthamiella* genus, described by Spegazzini in 1883, includes twelve species inhabiting the Andean and extra-Andean regions of Patagonia between 37° and 52° south latitudes. These species thrive in open steppe communities or on rocky-sandy soil at elevations from 300 to 1700 meters. Characterized by cushion-shaped shrub with small tubular flowers attached to the stem [7–9], *Benthamiella* belongs to the Solanaceae family, and together with *Pantacantha* and *Combera* genera, constitute the closely related Patagonian endemic and unstudied Benthamielleae tribe [10].

In Chile *B. azurella* grows in Sierra Baguales, Magallanes, Chile, at 50°S latitude, in open Andean steppe, at the border with Argentina. Exposed to extreme weather, include low rainfall, strong winds and low temperatures [1, 11, 12], this specie have small and geographically restricted populations, increasing their vulnerability [13]. The Chilean Environment Ministry classified it as vulnerable and endangered under Decree DS 13/2013 MMA.

The Solanaceae family contains diverse bioactive metabolites. The Patagonian solanaceae species, commonly contain flavonoids, phenolic acids, alkaloids [14], coumarins, terpenes [15], and steroidal saponins [16]. These plants exhibit strong antitumor activity against a variety of cell lines, often associated with withanolide-type steroids [17], steroidal saponins [16], and polysaccharides [18]. Solanaceae constituents also showed significant antimicrobial activity against a wide range of bacterial and fungal pathogens [19, 20]. Other family bioactivities include sedative-anxiolytic effects [14], insecticidal and antifeedant activity [15, 21, 22], gastroprotective effect and β -glucuronidase inhibitors [15].

The aim of this study was to conduct an unprecedented first exploration of the endemic Patagonian plant, *B. azurella*, through the analysis of biochemical composition, metabolites profiles, and bioactivities including antioxidant, antibacterial, *in-vitro* cytotoxicity, acute toxicity, and quorum quenching of its aerial and root parts.

2. MATERIALS AND METHODS

2.1 Solvents and reagents

Solvents and reagents used in GC-MS, IR, LC-MS, proximate, polyphenols and antioxidant analyses and extracts preparation were obtained in Sigma-Aldrich, St. Louis, MO, USA, except Tri-Silyl reagent (Thermo Fisher Scientific, Franklin, MA, USA). The cytotoxic analysis reagents were acquired in Biowest, Nuaille, France. The bacterial analysis reagents were obtained in Oxoid Ltd., Basingstoke, Hampshire, UK.

2.2 Biological material

Human colon cancer cell line HCT-116, hepatocyte cancer cell line HepG2 and immortalized human keratinocytes HACAT were purchased from American Type Culture Collection (ATCC, Manassas, VA, USA). Bacterial strains were obtained from the stock collection of the Microbiology Department at the University of Málaga.

2.3 Equipment and software

Gas chromatography Trace GC, autosampler Tri Plus and DSQ mass spectrometer quadrupole chromatographic column Zebron ZB-5, Phenomenex (30 m x 0.25 mm ID x 0.25 μ m) (Thermo Fisher Scientific, Franklin, MA, USA). UltraHigh-Performance Liquid Chromatography (UHPLC), compact QTOF mass spectrometer, chromatographic column Kenetex C18 (2.1 mm x 100 mm, particle size 1.7 μ m) (Phenomenex, Torrance, CA, USA). Metaboscape 4.0 software (Bruker, Billerica, MA, USA). Spectral library of MassBank of North America (MoNA, Davis, CA, USA). Freeze-dried (Telstar, Iyoquest). Vortex (Scilogex SCI-VS, Rocky Hill, EE.UU.). Thermo Nicolet Avatar 360 IR spectrophotometer + DTGS detector, OMNIC 7.2 software (Thermo Electron

Inc., Waltham, MA, USA). Elemental analyzer (LECO TruSpec Micro CNHS, St. Joseph, MI, USA). Muffle furnace (Vulcan, A550). Vortex (Sciologex SCI-VS, Rocky Hill, EE.UU). UV-spectrophotometer (Shimadzu, UV 160A, Japan). Microplate spectrophotometer (BIO-TEK, FL600, INC. Winooski, VT, USA). Luminometer (Microtox M500, Microbics Corporation, Carlsbad, CA, USA). GraphPad Prism 8.0.2 software (GraphPad, San Diego, CA, USA).

2.4 Vegetal material

B. azorella was collected in Sierra Baguales sector, in Magallanes, Chile, at 50.73°S, 72.39°W, 973 meters high in December 2022. Plant biomass was transported to the laboratory at 4°C, cleaned to remove impurities and botanically identified. The aerial parts (BA.AP) and root (BA.R) of *B. azorella* were separated, frozen at -40°C, freeze-dried, and ground into powder for biological and biochemical composition analysis.

2.5 Preparation of plant extracts

For metabolite profiling and cytotoxic *in vitro* analysis, extracts were prepared from 10 g of lyophilized BA.AP and BA.R powder in 100 mL of distilled water. The mixture was left at room temperature overnight with constant stirring, then centrifuged, and the supernatant was freeze-dried. For antibacterial analysis, samples were prepared from lyophilized BA.AP and BA.R powder in distilled

water and absolute ethanol to a concentration of 20 mg mL⁻¹, agitated with Vortex for 5 min, and used immediately.

2.6 Extraction and purification of polysaccharides

Polysaccharides (POL) were extracted from *B. azorella* using a modified method from Parages, 2012 [23] summarized in **Figure 1**. Initially, 20 g of lyophilized BA.R powder were depigmented with 400 mL of EtOH_{abs} with stirred at room temperature for 24 h, then centrifuged at 9000 rpm for 15 min, and supernatant discarded. This step was repeated three times until the supernatant was colorless. The pellet obtained was treated with 500 mL of H₂O, boiled for 1 h with constant stirring, cooled and centrifuged (9000 rpm x 15 min). The supernatant was separated from pellet and cooled to 4°C, placed in an ice bath, and an equal amount of cold EtOH_{abs} was added to achieve the crude POL precipitation. After standing for 12 h at 4°C, the mixture was centrifuged (9000 rpm x 15 min) and the supernatant was removed. The crude POL was purified by redissolving it in 200 mL of 4 M NaCl, stirred for 30 min at 60°C. The undissolved precipitate was discarded, and the POL precipitation process was repeated. The obtained precipitate was placed onto a dialysis membrane, immersed in a 0.5 M NaCl solution, and stirred overnight at room temperature. After dialysis, the membrane content was extracted, washed with EtOH_{abs} for total POL precipitation, cooled to -80°C and freeze-dried.

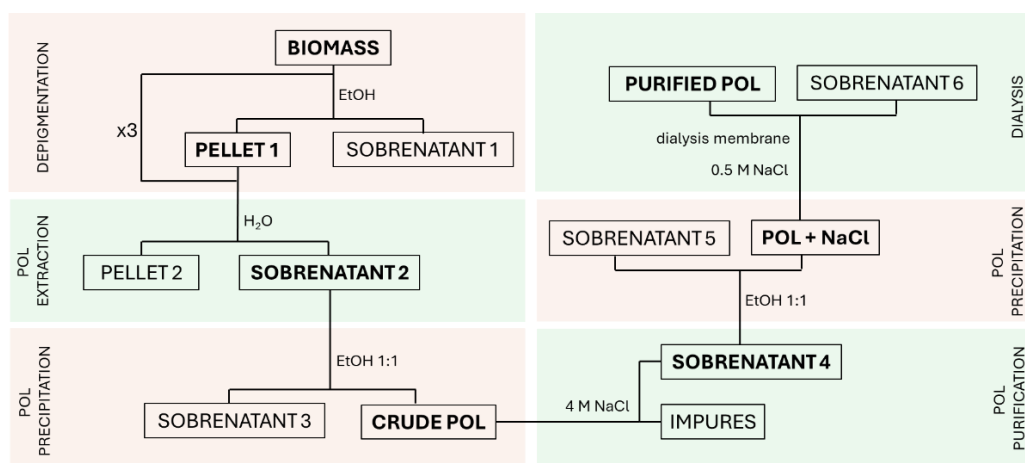


Figure 1: Scheme of polysaccharides extraction and purification.

2.7 Gas Chromatography-Mass Spectrometry (GC-MS)

2.7.1 Derivatization of polysaccharides: methanolysis and silylation

For the methanolysis, 600 µL of HCl in methanol 3 N were added to 2.32 mg of *B. azorella* roots polysaccharides (BA.R-POL) and heated for 24 h at 80°C. The solvent was evaporated under nitrogen stream, the residue was washed three times with methanol and dried to remove excess acid. The residue was then derivatized by silylation with 300 µL of Tri-Sil reagent for 1 h at 80°C. The derived sample was dried under nitrogen stream, extracted with 500 µL of hexane, centrifuged, the supernatant filtered, evaporated, and reconstituted in 150 µL of hexane LC-MS grade. Finally, silylated monosaccharides were analyzed in duplicate.

2.7.2 Monosaccharides GC-MS Analysis

GC-MS analysis was carried out using a gas chromatography Trace GC, autosampler Tri Plus, DSQ mass spectrometer quadrupole and column zebron ZB-5. The injection volume was 1 µL in splitless mode with a relation split of 30 at 250°C, with a helium flow rate of 1.2 mL per min. The initial column temperature was 80°C for 2 min, then ramped to 155°C at 5°C per min, to 158°C at 0.5°C per min and finally to 230°C at 5°C per min. The mass spectrometer operated in electron impact ionization (EI) mode at 70 eV, monitoring in full scan (50–600) and in single ion monitoring mode (204 and 217 m z⁻¹). Interface and ionization source temperature were 230°C. Derivatized monosaccharides were identified by comparing retention times and mass spectra with monosaccharides standards analyzed under identical conditions and the National Institute of Standards and Technology library.

2.8 Fourier Transform Infrared Spectroscopy (FT-IR)

For FT-IR analysis, a self-supporting disc (16 mm diameter) was made pressed (15 cm² for 2 min) a mixture of BA.R-POL and KBr (1% w/w) which was introduced in the IR spectrophotometer + DTGS detector for its characterization. The FT-IR spectra was obtained between 400–4000 cm⁻¹ region with a resolution of 4 cm⁻¹, OMNIC 7.2 software (bandwidth: 50 cm⁻¹; enhancement factor: 2.6) was used, baseline adjustment and smoothing were performed in each spectrum.

2.9 Biochemical Composition.

2.9.1 Total Internal Carbon, Nitrogen, Hydrogen and Sulphur

Total Carbon, Nitrogen, Hydrogen and Sulphur contents in BA.AP and BA.R dry powder were determined using an elemental analyzer in the Research Support Central Services of the University of Malaga. This equipment uses the total combustion technique of sample that converts carbon to CO₂, hydrogen to H₂O, nitrogen to N₂, and sulphur to SO₂. The combustion gases: carbon, hydrogen and sulphur were quantified by a selective IR absorption detector and nitrogen by differential thermal conductivity sensor, independently.

2.9.2 Ashes and organic matter

Inorganic Compounds (Ashes) were determined by combusting samples at 500°C for 12 h, eliminating all organic matter. Two grams of BA.AP and BA.R dry powder were placed into a pre-weighed crucible, combusted in a muffle furnace, cooled in a desiccator, and weighed. The experiment was performed in triplicate.

2.9.3 Proteins

Protein content was calculated by multiplying the total nitrogen percentage (from the elemental analyzer) by a plants global nitrogen-to-protein conversion factor (N-Prot) of 4.43 [24], since the specific factor for *Benthamiella* genus was not determined.

2.9.4 Carbohydrates

Carbohydrates were determined using the colorimetric method of Dubois et al. 1956 [25]. Briefly, 5 mL of 1 M H₂SO₄ was added to 5 mg of BA.R and BA.AP dry powder (in triplicated) and heated in a water bath at 100°C for 1 h. After cooling, 0.2-0.3 mL of the acid extract was separated from pellet by centrifugation at 4000 rpm at 10°C for 15 min, diluted to 1 mL with 1 M H₂SO₄, and mixed with 1 mL of 5% phenol. Finally, after 40 min at room temperature, the mixture was combined with 5 mL of concentrated H₂SO₄. Absorbance was measured at 485 nm in a UV-spectrophotometer. A blank was prepared similarly, and anhydrous glucose was used for calibration curve.

2.9.5 Lipids

Total lipids were determined using a modified Folch et al. 1957 method [26]. By triplicate, 200 mg of BA.AP and BA.R dry powder were homogenized in 5 mL of chloroform:methanol (2:1) with 0.01% butylhydroxytoluene. After adding 2 mL of KCl 0.88% and centrifuging at 2000 rpm for 5 min, the lipid fraction was separated, filtered, and the solvent evaporated under nitrogen flow. Gravimetric quantification was made according to **Equation 1**, where DW correspond to dried weigh:

$$\text{Lipids (\%)} = \left[\frac{\text{lipids (g)}}{\text{biomass (g DW)}} \right] \times 100 \quad (1)$$

2.10 Phenolic Compounds

Total Phenolic compounds were determined using a modified photocolometric Folin–Ciocalteu (FC) method [27]. with some modifications. By triplicate, 20 mg of BA.AP and BA.R dry powder were mixed with 1 mL of MeOH 80%, stirred, incubated for 12 h at 4°C in darkness, centrifuged, and the supernatant separated. One hundred microliter of supernatant was mixed with 700 µL of distilled water, 50 µL of Folin–Ciocalteu phenol reagent, and vortex. Then, 150 µL of Na₂CO₃ 20% was added, stirred, and incubated for 2 h at 4°C in darkness. Absorbance was measured at 760 nm using gallic acid as standard. To eliminate interferences, in a new analysis samples were pre-treated with polyvinylpyrrolidone (PVPP). Adsorbed phenols (AP) by PVPP were calculated by the difference in absorbance with and without PVPP, according to **Equation 2**:

$$\text{Abs(AP}_{\text{by PVPP}}) = \text{Abs(FC}_{\text{without PVPP}}) - \text{Abs(FC}_{\text{with PVPP}}) \quad (2)$$

2.11 Antioxidant capacity

Antioxidant capacity (AC) was evaluated using the ABTS and DPPH methods in triplicate. %AC was calculated according to **Equation 3**, where Abs₀ is absorbance at time 0 and Abs₁ at the end of reaction.

$$\text{AC\%} = [(Abs_0 - Abs_1) / Abs_0] \times 100 \quad (3)$$

The Half maximal inhibitory concentration (IC₅₀) was calculated using scavenging effect (%) versus extract concentration (µg mL⁻¹) and adjusted to a non-linear regression in GraphPad Prism Software.

2.11.1 DPPH method

The DPPH method, reported by Brand-Williams, et al. (1995) [28], was used with a few modifications. In brief, samples were extracted in 80% methanol for 30 min at 4°C in darkness. Then, 150 µL of samples (114-1818 µg mL⁻¹) were added to 1.5 mL of 0.125 mM DPPH (2,2-diphenyl-1-picrylhydrazyl) in 90% methanol. The mixture was incubated for 30 minutes at room temperature in darkness (end of reaction). Absorbances (Abs₀ and Abs₁) were measured at 517 nm. A pattern curve with DPPH at different concentrations and a calibration curve with ascorbic acid (0-30 µM) were performed. Antioxidant capacity was expressed as µmol of ascorbic acid equivalent (AAE) per g⁻¹ of DW.

2.11.2 ABTS method

The ABTS method, reported by Re, et al. [29], was used with a few modifications. In brief, ABTS radical cation (ABTS^{•+}) was generated by reacting 7 mM 2,2'-azino-bis (3-ethylbenzothiazoline-6-sulfonic acid (ABTS) with 2.45 mM potassium persulphate (K₂S₂O₈) in 0.1 mM PBS pH 6.5. The solution was stored for 12-16 hours at room temperature and diluted with PBS to adjust absorbance to 0.9-0.7 at 727 nm. Samples were incubated in PBS for 12 h at 4°C in darkness, centrifuged, and the supernatant separated. For analysis, 15 µL of sample at various concentrations were added to 285 µL of ABTS^{•+} and incubated for 8 minutes at room temperature in darkness (end of reaction). Abs₀ and Abs₁ were measured at 727 nm. A calibrate curve was made with 0-400 µM of Trolox (6-hydroxy-2,5,7,8-tetramethylchroman-2-carboxylic acid), and antioxidant capacity was expressed as µmol of Trolox equivalent (TE) per g⁻¹ of DW.

2.12 Cell culture

To the culture cell, three cell lines were used: human colon cancer HCT-116, hepatocyte cancer HepG2, and immortalized human keratinocytes HACAT. HCT-116 and HepG2 cell lines were cultured in Dulbecco's Modified Eagle's Medium (DMEM) and HACAT cell line in RPMI-1640 medium. Cells were supplemented with 10% fetal bovine serum, 5 mL penicillin-streptomycin solution 100X, 2 mM L-glutamine and 2.5 mL amphotericin B, incubated in a 96-well microplate at 37°C in humidified air with 5% CO₂, until 75-80% confluency, then, collected and centrifugated at 200 rpm for 5 min.

2.12.1 Cell Viability assay of tumoral lines

For cytotoxic analysis of *B. azorella* extracts, cell proliferation was estimated using the 3-(4,5-dimethylthiazol-2-yl)-2,5-diphenyltetrazolium bromide (MTT) assay [30]. Tumoral HTC-116 and HepG2 cell lines were individually incubated with serial dilutions of extracts (10 to 4.76x10⁻⁶ mg mL⁻¹) in a 96-well microplate for 72 h at 37°C with 5% CO₂. Control cells were incubated without treatment. Next, ten µL of MTT solution (5 mg mL⁻¹ in PBS) was added to microplate and incubated at 37°C for 4 h. Formed purple formazan crystals were solubilized with 150 µL of 0.04 N HCl in 2-propanol, except for HACAT (solubilized in DMSO) was measured at 550 nm using a microplate spectrophotometer. Determinations were performed in triplicate in independent experiments and *Cell viability (%)* was calculated according to **Equation 4**:

$$\text{Cell viability (\%)} = \left[\frac{\text{Abs}_{\text{treatment}}}{\text{Abs}_{\text{control}}} \right] \times 100 \quad (4)$$

Abs_{treatment} is the absorbance of the treated cells, and *Abs_{control}* is the absorbance of the control cells. The IC₅₀ was determined using a non-linear in GraphPad prism Software.

2.13 In vitro antibacterial activity

Three bacterial analyses were conducted: bacterial inhibition, acute toxicity, and quorum quenching assays For this, both, saline and ethanolic fresh stock solutions at concentration of 20 mg mL⁻¹ were prepared starting from lyophilized powder of BA.AP and BA.R separately, vortexing for 5 min and used immediately. Experiments were performed in triplicate, including negative control, and documented with photographs.

2.13.1 Bacterial inhibition

In the bacterial inhibition assay, various strains were used: one non-pathogenic (*Vibrio fischeri*), six humans pathogenic (*Enterococcus faecalis*, *Escherichia coli*, *Salmonella enterica*, *Staphylococcus aureus*, *Cutibacterium acnes* CECT 5684, and *Chromobacterium violaceum*), and four fish pathogenic (*Vibrio anguillarum* CECT 522, *Vibrio harveyi* Lg16/00, *Aeromonas hydrophila* Lg28/4, and *Photobacterium damsela* subsp. *Piscicida* Lg41/01). Each strain was cultivated under specific conditions (**Table 1**) using Trypticase soy agar (TSA), TSA with 2% NaCl (TSAs), Reinforced Clostridial Medium (RCM) culture media supplemented with 1.5% bacteriological agar (RCMA), and LB broth Miller with kanamycin antibiotic (LB+k). The well and disc diffusion methods, based on García-Márquez et al.[31] were used. Initially, bacterial strains were reseeded, incubated, and suspended in a 2% NaCl solution, adjusted to 0.5 McFarland turbidity, and plated on suitable culture media for their growth. Aqueous and ethanolic fresh solutions of *B. azorella* were analyzed. In the well

diffusion method, 6 mm diameter wells were cut into agar and filled with 100 μ L of aqueous solution. Saline solution was the negative control. In the disc diffusion method, 10 μ L of ethanolic extract was applied to sterilized filter paper

discs (6 mm diameter, Whatman no. 1). Ethanol was the negative control. After drying, discs were placed on agar plates and incubated. Antibacterial activity was assessed by the presence or absence of inhibition zones around each well or disc.

Table 1: Characteristics and working conditions of each bacterial strain used.

Type	Pathogenic or non-pathogenic	Gram	Strain	Culture medium*	Incubation conditions
human	pathogenic	(+)	<i>Enterococcus faecalis</i>	TSA	37°C 24h
			<i>Staphylococcus aureus</i>	TSA	37°C 24h
			<i>Cutibacterium acnes</i>	RCM	37°C 24-48h**
		(-)	<i>Salmonella enterica</i>	TSA	37°C 24h
			<i>Escherichia coli</i>	TSA	37°C 24h
			<i>Chromobacterium violaceum</i>	LB+K	30°C 24h
fish	non-pathogenic		<i>Vibrio fischeri</i>	TSAs	22°C 24-48h
	pathogenic	(-)	<i>Vibrio anguillarum</i>	TSAs	22°C 24-48h
			<i>Vibrio harveyi</i>	TSAs	22°C 24-48h
			<i>Aeromonas hydrophila</i>	TSAs	22°C 24-48h
			<i>Photobacterium damsela</i> ***	TSAs	22°C 24-48h

* Trypticase soy agar (TSA), TSA with 2% NaCl (TSAs), Reinforced Clostridial Medium (RCM), bacteriological agar (RCMA), LB broth Miller with kanamycin antibiotic (LB+k). ** Anoxic conditions. *** *Subsp. Piscicida*

2.13.2 Acute toxicity

The acute toxicity tests were conducted using a luminometer as described by García-Márquez et al. [31]. This method assesses the inhibition of bioluminescence of *V. fischeri*, indicating potential toxicity. Briefly, Samples were prepared by serial dilutions of fresh aqueous stock solutions of *B. azorella* dry powder, ranging from 1000 to 1.95 μ g mL⁻¹. A Fresh *V. fischeri* suspension (0.7 optical density at 600 nm) was prepared and maintained at 5°C. Then, 20 μ L of *V. fischeri* was added to a cuvette containing 1 mL of the sample at different concentrations. The mixture was incubated at 15°C for 15 min, and bioluminescence was measured. The decrease in bioluminescence was calculated relative to the control (*V. fischeri* in 2% NaCl solution).

2.13.3 Quorum quenching

Quorum quenching activity was performed according to Ibrahim et al. [32] with modifications, focus on identifying compounds that disrupt the acyl homoserine lactone (AHL) signaling pathway—a critical component of quorum sensing process. *V. fischeri* was used as the AHL-producing bacterium, and *Ch. violaceum* CV026 (NCTC 13278) served as biosensor of AHLs. *Ch. violaceum* was grown on an LB+k culture medium plate. A concentrated *V. fischeri* spot was placed on the plate. Then, 100 μ L of saline stock solution were poured directly onto the *V. fischeri* spot. For ethanolic solutions, 10 μ L were applied to a disc, solvent evaporated, and placed on the bacterial spot.

2.14 UPLC-MS analysis

Metabolites in *B. azorella* extract were tentative identification using UPLC + QTOF MS. To obtain the extracts, 10 g of lyophilized BA.R powder was added to 100 mL of distilled water and stirring overnight at room temperature. The solution was centrifuged, and the supernatant was freeze-dried. The extract was dissolved in 1 mL methanol, transferred to an HPLC vial, and kept at 6°C. Chromatographic separation was performed using a Kenetex C18 column at 40°C with a flow rate of 0.4 mL min⁻¹. Five microliters of sample were injected. Mobile phases were 0.1% formic acid in water (A) and 0.1% formic acid in 90% acetonitrile (B). The gradient was: 88% A for 1 min, 88% to 1% A over 10 min, 1% A for 2.5 min, 1% to 88% A over 0.5 min, and 88% A for 1 min. Mass spectrometry data were acquired over a range of 50-1300 m/z in negative and positive ion modes of the electrospray ionization (ESI) source, sheath gas: 30 psi; auxiliary gas: 13; spray voltage: 3 kV; capillary temperature: 350°C; S-Lens RF level: 50; heater temperature: 150°C. The total separation time was 17 min. Data analysis was performed with Metaboscape 4.0 software using mass, fragmentation pattern, and isotopic pattern. MoNA spectral library was used for metabolite identification.

2.15 Statistical analysis

Analyses were performed in triplicate and results were presented as means \pm standard deviation (SD). Figures and statistical analyses were performed using GraphPad Prism software, ordinary one-way ANOVA multiple comparison was

performed, followed by a Tukey's post hoc test when significant differences were detected. Differences were considered statistically significant when $p < 0.05$.

3. RESULTS AND DISCUSSION

Characterizing *B. azorella* roots polysaccharides, enhances understanding of its biochemical features. The thermal, water-related, and solar stress to which *B. azorella* is exposed could favor a specific production of polysaccharides in the cell wall intended to protect the plant, as suggested by previous studies on water stress-tolerant plants [33, 34]. Structural analysis of these polysaccharides using IR and GC-MS is crucial for fully understanding the structure-function relationship and harnessing their potential in various applications.

3.1 GC-MS Analysis

This study examines the monosaccharide composition of BA.R-POL, as shown in Table 2, with the corresponding GC-MS spectrum presented in Figure 2. Gas Chromatography-Mass Spectrometry (GC-MS) is a powerful analytical method used to separate and identify the compounds within a sample, providing a detailed understanding of its chemical makeup [35, 36]. The analysis reveals that arabinose is the dominant monosaccharide in BA.R-POL, indicating its critical contribution to the sample's structural and functional properties. The substantial mass percentage of arabinose (30.57%) suggests that it plays a significant role in shaping the polysaccharide composition, which could have a major impact on the sample's biochemical characteristics [37, 38]. Though rhamnose is present in smaller amounts (5.94%), it may still be important for the biological activity of BA.R-POL. Its relatively low abundance compared to arabinose suggests that it may serve a more specific functional role, rather than being a major structural component [36, 37]. Galactose, which comprises 12.72% of the monosaccharide content, is likely to facilitate interactions with other biomolecules, particularly through glycosylation processes, which are essential for numerous biological functions [35, 36]. Glucose, a key monosaccharide and a primary energy source in many biological systems, is also present in significant amounts (27.58%), suggesting that it may be an important constituent of the polysaccharides in BA.R-POL [35, 36]. Additionally, the presence of galacturonic acid (23.18%), a common component of pectins, indicates the presence of polysaccharides involved in maintaining the structural integrity of plant cell walls.

Table 2: Content of monosaccharides in BA.R-POL.

<i>Benthamiella azorella</i> roots polysaccharides				
N°	Monosaccharide	Retention time (min)	Peak area	% Mass
1	Arabinose	18.32	166423268	30.57
2	Ramnose	19.19	38512377	5.94
3	Galactose	28.02	78209048	12.72
4	Glucose	29.55	167472287	27.58
5	Galacturonic acid	29.11	136274450	23.18

The high percentage of galacturonic acid highlights its possible key role in the functional properties of BA.R-POL [35, 37]. Overall, the combination of GC-MS analysis and monosaccharide content provides critical insights into the biochemical composition of BA.R-POL. The significant presence of arabinose, glucose, and galacturonic acid suggests a complex polysaccharide structure that may enhance the sample's functional properties [36, 37]. These results form a

foundation for further investigation into the biological activity and potential applications of BA.R-POL in fields such as nutrition, pharmacology, and biotechnology. The intricate biochemical profile of this species emphasizes the need for additional research to fully uncover its functional and biological implications [35, 37].

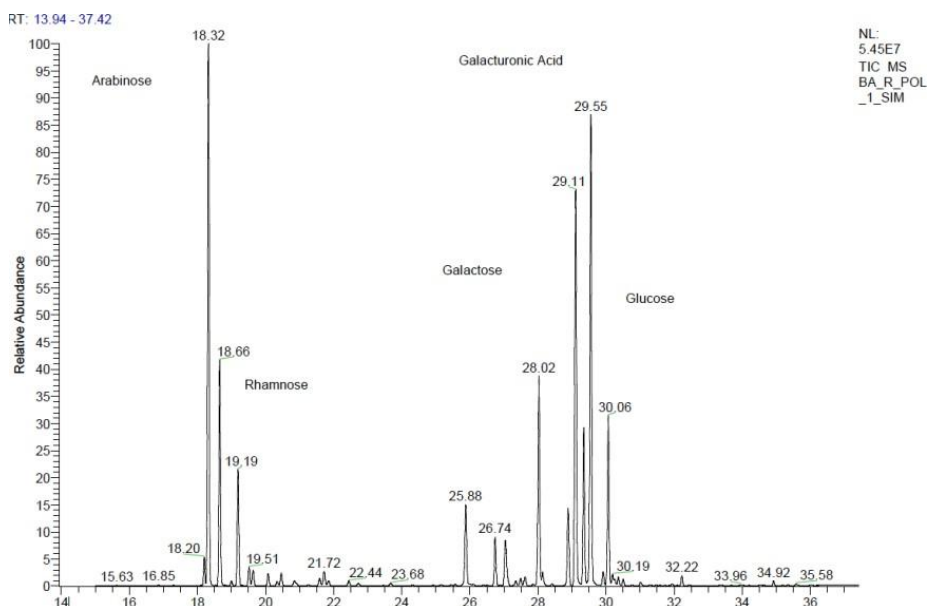


Figure 2: GC-MS spectrum of *B. azorella* roots polysaccharides (BA.R-POL).

3.2 Fourier Transform Infrared Spectroscopy (FT-IR)

The FT-IR spectrum of polysaccharides extracted from *B. azorella* (BA.R-POL) was recorded in the 4000-400 cm^{-1} region and is displayed in Figure 3. The spectrum reveals a complex array of absorption bands corresponding to various functional groups typical of polysaccharides. Peaks at approximately 3298 cm^{-1} , 2919 cm^{-1} , and 2886 cm^{-1} are associated with hydroxyl ($-\text{OH}$) and methylene ($-\text{CH}_2$) stretching vibrations, which are commonly found in polysaccharide structures [39, 40]. Specifically, the peak at 2919 cm^{-1} is attributed to asymmetrical stretching of the $-\text{CH}_2$ groups, while the peak at 2885 cm^{-1} corresponds to symmetrical stretching [41, 42]. The broad band near 3392 cm^{-1} suggests the presence of inter- and intramolecular hydrogen bonding, a characteristic feature in polysaccharides that contributes to their structural stability and solubility [39, 40]. The BA.R-POL spectrum

also indicates the presence of galacturonic acid-related functional groups, typically observed between 1700-1600 cm^{-1} , which confirms the acidic nature of the polysaccharide through the presence of carboxylate ions [43]. Notably, the carboxyl ($-\text{COOH}$) groups, characteristic of galacturonic acid, exhibit absorption around 1635 cm^{-1} [44]. These functional groups are crucial for the polysaccharide's gel-forming ability and interactions with biomolecules, making it useful in food and pharmaceutical applications [45]. Additionally, the peaks at 1418 cm^{-1} and 1370 cm^{-1} correspond to C-H bending vibrations, further indicating the presence of aliphatic groups within the polysaccharide structure [40, 46]. These features are important for understanding the molecular interactions and structure of the polysaccharide. Moreover, the peaks at 1314 cm^{-1} , 1249 cm^{-1} , and 1225 cm^{-1} represent C-O stretching vibrations, crucial for characterizing the glycosidic bonds in polysaccharides [40, 47].

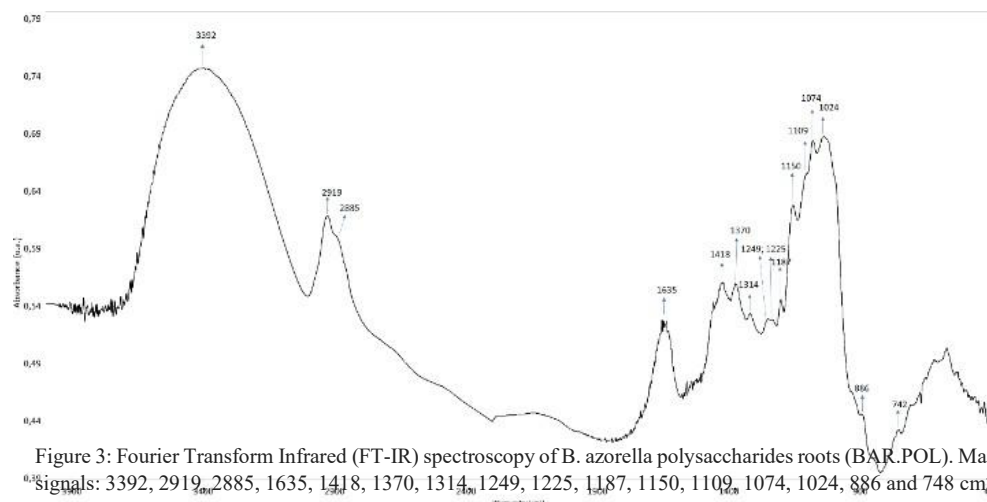


Figure 3: Fourier Transform Infrared (FT-IR) spectroscopy of *B. azorella* polysaccharides roots (BA.R-POL). Main signals: 3392, 2919, 2885, 1635, 1418, 1370, 1314, 1249, 1225, 1187, 1150, 1109, 1074, 1024, 886 and 748 cm^{-1} .

suggesting the presence of various monosaccharides like glucose, galactose, or mannose, which contribute to the functional properties of BA.R-POL [48]. The peaks at 1187 cm^{-1} , 1150 cm^{-1} , and 1109 cm^{-1} are also significant as they indicate

C-O-C stretching vibrations characteristic of glycosidic linkages [46, 49]. The peak at 1074 cm^{-1} suggests the presence of pyranose rings, confirming the polysaccharide nature of the sample [47, 49]. Finally, the peaks at 1024 cm^{-1} ,

886 cm^{-1} , and 748 cm^{-1} may suggest specific structural motifs such as anomeric carbons or other functional groups, which play a crucial role in the biological activity of polysaccharides [50, 51]. In particular, the 886 cm^{-1} peak is often associated with anomeric CH in β -galactose residues, highlighting asymmetrical stretching [52]. These findings align with the monomeric composition analysis by GC-MS, suggesting that BA.R-POL exhibit a diverse range of functional groups, potentially contributing to their applications in food, pharmaceutical, and cosmetic industries [53]. In conclusion, the FTIR analysis of BA.R-POL reveals a complex polysaccharide structure, providing essential insights into their structural and functional properties. These results pave the way for further in-depth structural studies of BA.R-POL.

3.3 Biochemical Composition

The biochemical composition of *B. azorella* aerial parts and roots was determined. **Table 3** shows the elemental analysis results, including total carbon, nitrogen, and sulphur content. The aerial parts exhibited higher Carbon (50.93%) and Hydrogen (6.98%) than the roots. In contrast, the Nitrogen percentage was slightly higher in roots (0.61%). Interestingly No Sulphur was detected in the plant. The molar ratio of Carbon to Nitrogen C:N was higher in the aerial parts (116.48) than roots.

Generally, elemental analysis revealed similar concentrations between aerial parts and roots of *B. azorella*. Carbon percentage is higher than in some algae [30, 54] and plants [55, 56], but lower than in certain microalgae [57]. In contrast, the previous authors report higher nitrogen percentage in their study organisms, resulting by comparison in a high C/N molar ratio for *B. azorella*. Interestingly, sulfur was undetectable using elemental analysis, likely due to low bioavailability in the steppe soils (1.6-4 mg kg^{-1}) [58].

Table 3: Content of total Carbon, Hydrogen, Nitrogen, Sulphur and molar ratio of Carbon to Nitrogen C:N in *B. azorella* aerial parts and roots (BA.AP and BA.R). Values are expressed as % relative to dried weight (DW) of sample, as average \pm SD (n=3).

	<i>Benthamiella azorella</i>	
	Aerial parts	Roots
Carbon	50.93 \pm 0.00	45.18 \pm 0.02
Hydrogen	6.98 \pm 0.15	6.09 \pm 0.23
Nitrogen	0.51 \pm 0.09	0.67 \pm 0.07
Sulphur	0.00 \pm 0.00	0.00 \pm 0.00
C:N	116.48	79.18

Respect to the proximate analysis, the content of ashes, carbohydrates, proteins, and lipids was analyzed. Organic matter was calculated by subtracting ash content, and fiber by subtracting lipids, proteins, and carbohydrates to the organic matter content. The results obtained for *B. azorella* align with findings in certain solanaceae plants [59]. **Table 4** reports almost double of ash in roots compared to aerial parts. Carbohydrates were highest, in roots more than twice as much as aerial parts. Lipid content in aerial parts was 4.57 times higher than in roots, consistent with observations on membrane composition of plants exposed to cold and drought stress. Specifically, decreased temperature correlates with increased unsaturated fatty acid content [60].

Table 4: Content of organic matter, ashes, carbohydrates, proteins, and lipids. Values are expressed as % relative to DW of sample, as average \pm SD (n=3).

		<i>Benthamiella azorella</i>	
		Aerial parts	Root
ASHES		11.66 \pm 0.88	19.14 \pm 3.50
	Total organic matter.	88.34 \pm 0.88	80.86 \pm 3.50
	Fiber	58.73	37.45
ORGANIC MATTER	Carbohydrates	15.73 \pm 0.05	37.90 \pm 0.13
	Proteins	2.26 \pm 0.09	2.97 \pm 0.07
	Lipids	11.62 \pm 0.65	2.54 \pm 0.07

The total phenolic compounds content in BA.AP and BA.R measured using the Folin-Ciocalteu method in absence of PVPP, and the adsorbed phenols by

presence of PVPP were measured in triplicated and the results are shown in **Table 5**. Roots had the highest total phenolic compounds (6.66 $\text{mg eq gallic acid (GAE)}$ per g of dried weight (DW)). Using PVPP, interferences were identified (88 to 77%), the highest adsorbed phenols was in roots (1.56 mg GAE g^{-1} DW), exceeding those reported for some *Holigarna* species [61], but not matching levels observed in certain *Nothofagus* and *Berberis* species from Patagonia [62].

Natural Polyphenols have attracted interest in the search of new drugs due to their potential as antioxidants and likely low toxicity, even at high concentrations [63, 64]. Notably, the Folin-Ciocalteu method may overestimate total phenolic content due to interference from non-phenolic reducing agents. The PVPP selectively adsorbs phenols, leaving interfering substances (such as aromatic amines, organic acids, reducing sugars, sulfates and sulfites) in solution [65]. In our tested samples, this interference was notably high, consistent with findings in other studies [66]. It's important to consider that under the tested conditions, some unadsorbed polyphenols may remain alongside the interferents; successive PVPP additions could mitigate this error [67].

Table 5: Content of Total phenolic compounds and Adsorbed phenols (by PVPP) expressed as “mg eq gallic acid (GAE) g^{-1} dried weight (DW)”, as average \pm SD (n=3).

	<i>Benthamiella azorella</i>	
	Aerial parts	Roots
Total phenolic compounds	5.50 \pm 0.28	6.66 \pm 0.62
Adsorbed phenols (by PVPP)	0.65 \pm 0.38	1.56 \pm 0.65
% interferences	88.18 \pm 1.80	76.58 \pm 0.45

3.4 Antioxidant capacity

3.4.1 DDPH method

The antioxidant activity of BA.R and BA.AP extracts using DPPH method are shown in **Figure 4**. The IC_{50} of root extract was 717.2 $\mu\text{g mL}^{-1}$. The maximum antioxidant capacity of roots was 89.43 \pm 0.74 $\mu\text{mol AAE g}^{-1}$ DW (76.77 \pm 0.63%) at 1818 $\mu\text{g mL}^{-1}$. Aerial parts had a maximum antioxidant capacity of 25.15 \pm 3.24 $\mu\text{mol AAE g}^{-1}$ DW (21.59 \pm 2.78%) at the same concentration. Significant differences were found between roots and aerial parts, except at 114 $\mu\text{g mL}^{-1}$. Ascorbic acid standard IC_{50} was 18.65 $\mu\text{g mL}^{-1}$.

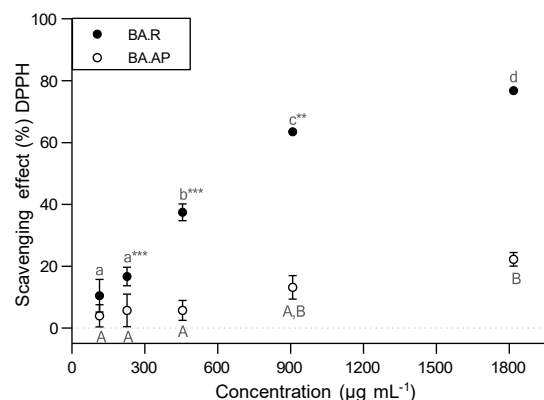


Figure 4: Comparative scavenging effects (%) of BA.R and BA.AP extracts at 0-1818 $\mu\text{g mL}^{-1}$ using DPPH method. Data are average \pm SD (n=3). Similar letters indicate no significant differences (Tukey, $p < 0.05$) between the different concentrations. * $p < 0.05$ -0.01; ** $p < 0.01$ -0.005; *** $p < 0.005$ -0.001.

3.4.2 ABTS method

The antioxidant activity of BA.R and BA.AP extracts using ABTS method are shown in **Figure 5**. The IC_{50} of roots and aerial parts were 511.2 $\mu\text{g mL}^{-1}$ and 528.7 $\mu\text{g mL}^{-1}$, respectively. Roots had a maximum antioxidant capacity of 1336.83 \pm 51.25 $\mu\text{mol TE g}^{-1}$ DW (84.97 \pm 3.25%) at 500 $\mu\text{g mL}^{-1}$. Aerial parts had 948.69 \pm 52.80 $\mu\text{mol TE g}^{-1}$ DW (60.30 \pm 3.36%) at the same concentration. Significant differences were found between roots and aerial parts at concentrations of 62.5 to 500 $\mu\text{g mL}^{-1}$. Trolox standard IC_{50} was 97.030 $\mu\text{g mL}^{-1}$.

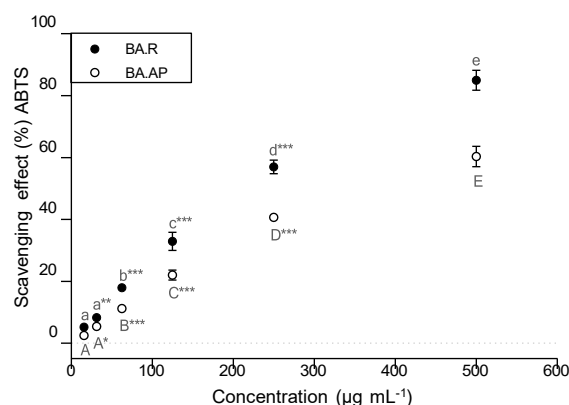


Figure 5: Comparatively scavenging effects (%) of BA.R and BA.PA extracts at 0-500 $\mu\text{g mL}^{-1}$ using DPPH method. Data are average \pm SD (n=3). Similar letters indicate no significant differences (Tukey, $p < 0.05$) between concentrations. * p 0.05-0.01; ** p 0.01-0.005; *** p 0.005-0.001.

Reactive oxygen and nitrogen species (RONS) are crucial metabolic byproducts for living organisms [68]. Imbalance between their generation and neutralization can lead to diseases and aging [69]. Using DPPH and ABTS assays, were observed higher antioxidant capacity in BA.R compared to BA.PA, consistent with dichloromethane extract of *Crotalaria burhi* [70], but contrary to hydro-methanolic extract of *Ruba tinctorum* [71]. The positive correlation between total phenolics and antioxidant capacity aligns with existing literature [72–74]. Due to the complexity of redox processes in living organisms, multiple methods are employed to assess antioxidant capacity (CA) and a perfect correlation among these is not always observed [68]. Notably, significant differences were found in the AC of *B. azurella* using DPPH and ABTS assays. Moreover, within the same method, there is significant variability in experimental conditions and results presentation [75, 76], which limits the comparison with other studies. Collection condition [73, 77] and processing of sample are factors that affecting AC. *B. azurella* was collected in late spring during the final flowering stage and dried via lyophilization, enhancing AC compared to air drying [72]. Some species are known to change their metabolite production and AC as a defense against oxidative stress in adverse environments [78, 79]. The intermittent drought, cold, and wind exposure likely affect the production of *B. azurella* antioxidant metabolites. However, its AC, analyzed by DPPH and ABTS, is lower compared to some Patagonian species (IC_{50} : 20–90 $\mu\text{g mL}^{-1}$) [62] or *Cestrum nocturnum*, of the same family (IC_{50} : 21–185 $\mu\text{g mL}^{-1}$) [80]. This study is the first to analyze AC in this species and its closest clade, highlighting the need for further experiments under well-defined conditions to achieve more robust results.

3.5 Cytotoxic activity

3.5.1 Cell viability of tumoral lines

Cytotoxic effect of BA.AP-H₂O, BA.R-H₂O and BA.R-POL extracts at different concentrations was estimated by MTT assays in HCT-116 and HepG2 cell lines.

For the colon cancer HCT-116 cell line (Figure 6), BA.R-H₂O extract showed the highest cytotoxic effect with an IC_{50} of 109.0 mg mL^{-1} (Figure 6A), cell proliferation was significantly ($p < 0.01$) reduced by BA.R-H₂O between 19.53–78.13, and 312.5–1250 $\mu\text{g mL}^{-1}$. No significant differences ($p > 0.05$) were observed between 78.13–156.25, 156.25–312.5, and 1250–10000 $\mu\text{g mL}^{-1}$. By Comparing, BA.AP-H₂O extract had a lower cytotoxic effect with a IC_{50} of 1089 mg mL^{-1} (Figure 6B), cell proliferation was significantly ($p < 0.01$) reduced by BA.R-H₂O at concentrations between 625–2500 and 5000–10000 $\mu\text{g mL}^{-1}$. BA.R-POL extract (Figure 6C) shows the lowest cytotoxic effect, there were no significant differences ($p > 0.05$) between 19.53–39.07, 39.07–2500, 312–5000 and 5000–10000 $\mu\text{g mL}^{-1}$. IC_{50} could not be calculated at the evaluated concentration.

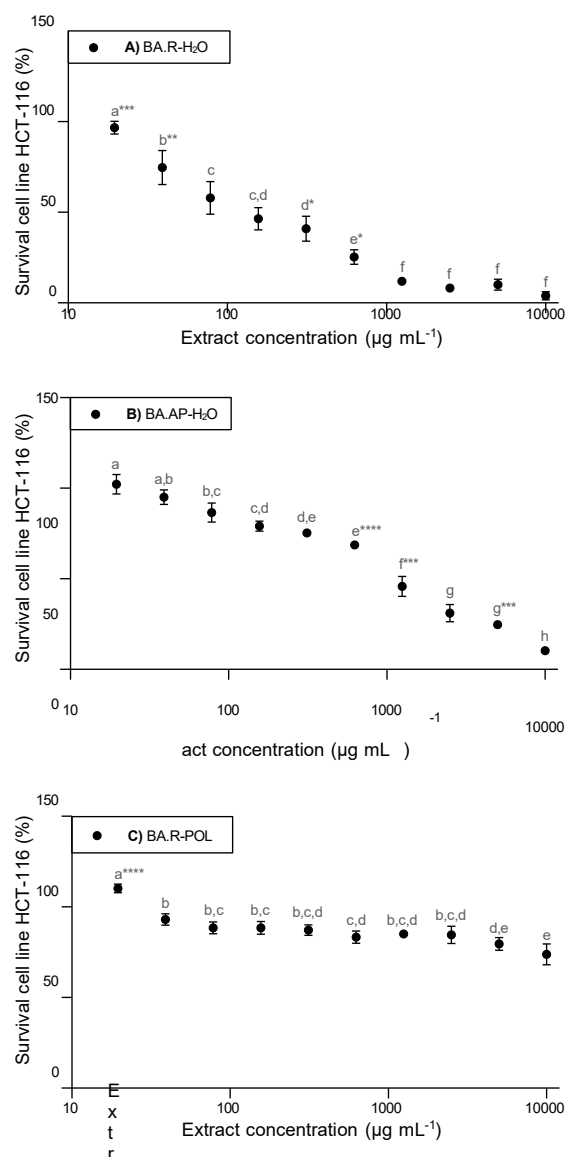


Figure 6: Survival HCT-116 cell line (%) incubated with A) BA.R-H₂O, B) BA.AP-H₂O and C) BA.R-POL extracts at 19.53-10000 $\mu\text{g mL}^{-1}$. Data are average \pm SD (n=3). Similar letters indicate no significant differences (Tukey, $p < 0.05$) between concentrations. * p 0.05-0.01; ** p 0.01-0.005; *** p 0.005-0.001.

The BA.R-POL extract cytotoxicity on hepatocytes cancer HepG2 cell line was evaluated (Figure 7). Results showed a lower cytotoxic effect with an IC_{50} of 1456 \pm 5.5 mg mL^{-1} . Cell proliferation was significantly ($p < 0.01$) reduced at 39.07–78.13 and 625–150 $\mu\text{g mL}^{-1}$.

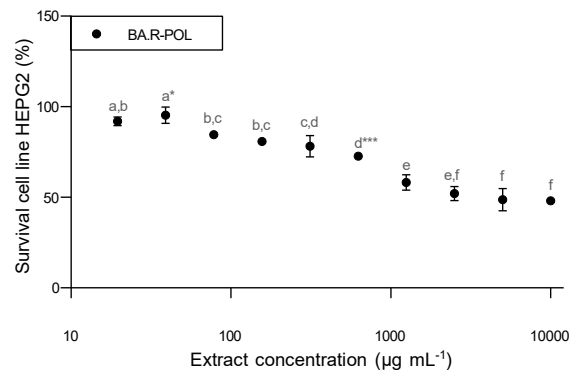


Figure 7: Survival HepG2 cell line (%) incubated with BA.R-POL extract at 19.53-10000 $\mu\text{g mL}^{-1}$. Data are average \pm SD (n=3). Similar letters indicate no

significant differences (Tukey, $p < 0.05$) between concentrations. * p 0.05-0.01; ** p 0.01-0.005; *** p 0.005-0.001.

Numerous studies link the anticancer activity of polysaccharides and polyphenols in natural products to their antioxidant properties [81]. In this regard, plants are a significant source of anticancer drugs [82]. This research first analyzed the anticancer activity of a *Benthamiella* specie, showing cytotoxicity against two tumor cell lines. For the HCT-116 colon cancer cell line, the BA.R-H₂O extract was most active, showing greater cytotoxicity than herbal infusions from six Patagonian species against the T84 colon cancer cell line, where the lowest EC₅₀ was 160 $\mu\text{g mL}^{-1}$ for *Solidago chilensis* [83]. The ethanolic extract of *Physalis angulata* leaves, from the same family as *B. azurella*, showed higher cytotoxic activity against HCT-116 with an IC₅₀ of 15.7 $\mu\text{g mL}^{-1}$ [84]. The BA.AP-H₂O extract showed mild activity (10 times lower than BA.R-H₂O) but still comparable to the cytotoxic activity of five of the six previously mentioned herbal infusions [83]. In contrast, BA.R-POL showed negligible cytotoxicity for this tumor line, suggesting that the activity of BA.R-H₂O is due to polar molecules different of polysaccharides. Unlike the minimal cytotoxicity of BA.R-POL against HCT-116, this extract showed higher activity against HepG2 hepatocellular carcinoma, with an IC₅₀ of 617.8 $\mu\text{g mL}^{-1}$, similar to the essential oil of *Datura metel*, with IC₅₀ value of 341.1- 613.8 $\mu\text{g mL}^{-1}$ [84]. Higher cytotoxicity (IC₅₀ between 5-25 $\mu\text{g mL}^{-1}$) has been found in extracts of *Withania* [85] and *Physalis* [86], genera of the same family. A study on the cytotoxic mechanism of bioactive compounds from Solanaceae showed that some might be effective against more than one type of cancer [87]. Therefore, analyzing BA.R and BA.AP extracts against HepG2 and other cancer cell lines will be of great interest for future research.

3.5.2 Cell viability of healthy line

Cytotoxic effect of BA.AP-H₂O, BA.R-H₂O and BA.R-POL extracts at different concentrations was estimated by MTT assays in healthy keratinocyte HACAT cell line (Figure 8). None of the extracts showed toxicity against HACAT cell line; they even slightly promoted cell growth. IC₅₀ could not be calculated.

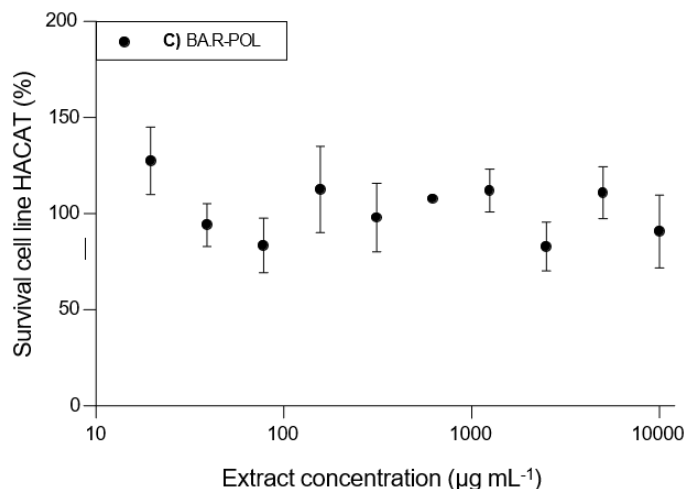
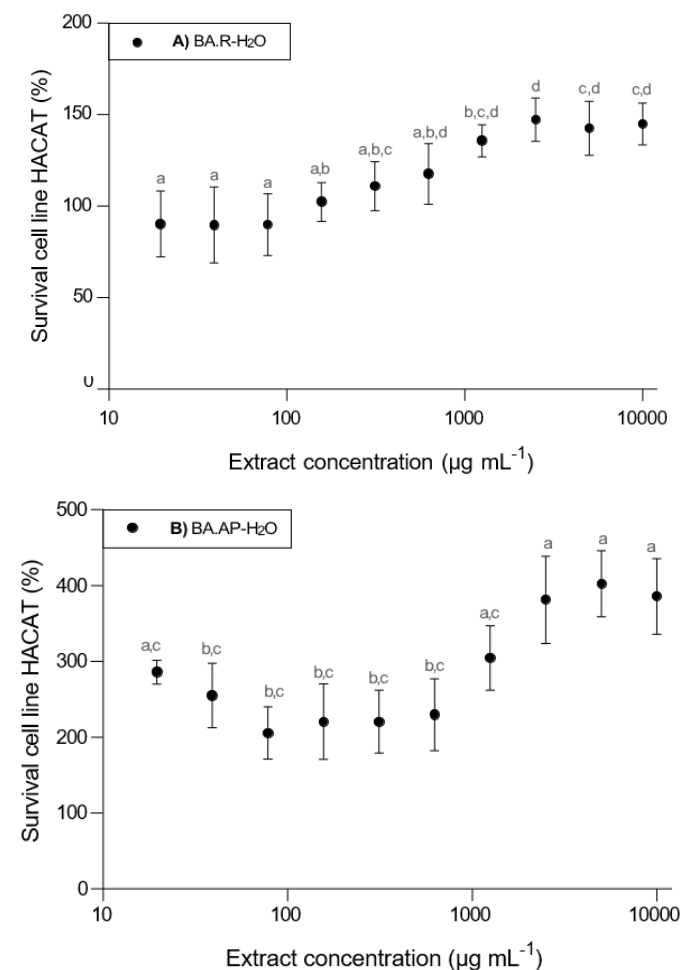


Figure 8: Survival HACAT cell line (%) incubated with A) BA.R-H₂O, B) BA.AP-H₂O, C) BA.R-POL extracts at 19.53-10000 $\mu\text{g mL}^{-1}$. Data are average \pm SD (n=3). Similar letters indicate no significant differences (Tukey, $p < 0.05$) between concentrations.

The healthy HACAT cell line is used to search for extracts or metabolites with pharmacological properties skin related. Some Aloe species enhance HACAT cell proliferation, aiding wound healing [108]. Moreover, HACAT inhibitors are of interest for treating hyperproliferative lesions, such as psoriasis vulgaris [109]. Polysaccharides and aqueous extracts of *B. azurella* exhibited no cytotoxic effect on HACAT cell lines. Results varied significantly between replicates, but BA.R-H₂O extract consistently increased cell proliferation in a concentration-dependent manner, reaching 147% viability at 2500 $\mu\text{g mL}^{-1}$. BA.AP-H₂O extract exhibited abnormal behavior, with cell viability exceeding 200% at all concentrations, while BA.R-POL extract did not affect the normal HACAT cell growth. Similar to *B. azurella* aqueous extracts, Smilax china floral extract at 150 $\mu\text{g mL}^{-1}$ increased cell viability to 200%, relative proliferation to 180%, and relative migration to 280% [110].

3.6 Bacterial inhibition, quorum quenching and acute toxicity.

Various Solanaceae species have shown variable sensitivity to human gram-positive and gram-negative bacteria, with MICs of extracts or metabolites ranging from 5 to 0.015 mg mL⁻¹ [20, 88, 89]. *B. azurella* bacterial inhibition assays indicate no activity at tested concentrations: 2 mg of plant lyophilized powder (corresponding to 80-50 μg of aqueous extract) per well and 0.2 mg of plant lyophilized powder (7-5 μg of ethanolic extract) per disc at tested strains, (relatively low compared with other family studies). New experiments at higher concentrations might reveal some activity. Studies on Patagonian plants show that Berberis microphylla alkaloid extract has significant activity against gram-positive bacteria with MICs between 333-83 $\mu\text{g mL}^{-1}$ [90], and Adesmia boronioides exudate has MICs between 128-16 $\mu\text{g mL}^{-1}$ against four pathogenic bacteria [91]. Higher concentrations should be tested.

Quorum sensing (QS) is a communication system among microorganisms that regulates behaviors like virulence and antibiotic resistance through chemical signals [92, 93]. Anti-QS strategies combat multi-resistance without antibiotics [94] and also have applications in agriculture, aquaculture, and the environment [92]. Natural products, including fungi, bacteria, and plants, are promising candidates [92, 95, 96]. *B. azurella* extracts showed no Anti-QS activity at tested concentrations (80-50 μg of aqueous extract and 7-5 μg of ethanolic extract). Comparatively, curcumin and some algae extracts inhibit QS at 50-25 mg mL⁻¹ [54] y 0.1 mg mL⁻¹, respectively [97].

The bioluminescence inhibition assay using *V. fischeri* bacterium is a simple, reproducible, and effective method for assessing the toxicity of water bodies [98], industrial effluents [99, 100], and organic molecules in aquaculture [101]. Acute toxicity test of *B. azurella* at 1 mg mL⁻¹ of lyophilized plant resulted in approximately 100% bioluminescence, indicating minimal toxicity. Thus, determining their IC₅₀ value was unfeasible.

3.7 LC-MS analysis

The tentative identification of metabolites in the most active extract: BA.R-H₂O, is detailed in Table 6 and 7. Positive ionization (Table 6) detected 1126 signals, with 82 linked to molecular formulas. Nine were tentatively identified

via databases and previously reported in natural products. Negative ionization (Table 7) detected 451 signals, with 53 linked to molecular formulas. Eleven were tentatively identified via database and previously reported in natural products. In total 4 derivatives coumarins, 3 terpenes, 2 steroidal sapogenins, 1 steroid, 1 hormone, 4 cinchona alkaloids, 2 phenols, 2 fatty acids, and 1 organic acid, were tentatively identified and associated with a wide variety of biological activities, principally antioxidant, anti-inflammatory, antimicrobial, anticancer, neuroprotective, and cardioprotective.

Metabolomic analysis provides valuable information on metabolites in organisms, including plants. It has applications in disease diagnosis, understanding adaptive processes, among others [102]. Using LC-MS, in total, fifteen molecular formulas linked to isomers of natural origin with biological activities were suggested for the most active of the studied extracts (BA.R-H₂O). Similarly, the most active extract from selected Solanaceae species underwent LC-MS analysis, identifying twelve known hydroxycinnamic acid, amides, steroid, alkaloids and derivatives [88]. Simple hydroxycoumarins, specially scopoletin, are common constituents in Solanaceae family [10]. This structural group was abundant in *B. azurella*, with scopoletin as the principal isomer, associated with antioxidant, anticancer, neuroprotective, and antimicrobial activities. Common Steroid sapogenin of spirostane and furostane derivatives occurring in Solanaceae [10]. In *B. azurella*, two spirostane derivatives, diosgenin and ruscogenin were found.

As in *B. azurella*, alkyl hydroxycinnamates (include ferulic acids) has been described in the lipid barrier of many plant species, with antioxidant and allelochemical properties [103]. LC-MS identified two triterpene isomers C₃₀H₄₈O as a 3-deoxyhopanoids. Three-hydroxy and 3-keto forms have been found in higher plants, but 3-deoxyhopanoids are typical in bacteria [104]. Given this evidence, it is more likely that they correspond to pentacyclic triterpenoid of oleanane and lupane derivatives (amyrenone or lupenone isomers) typical of the Solanaceae family [10, 105]. Loliolide, a carotenoid present in many plants, including *Solanum* (Solanaceae) [106], is a potential herbivore resistance inducer [107], with neuroprotective and anti-inflammatory properties [108, 109]. C₂₇H₄₂O was identified as a cholesterol derivative, previously found in *Milletia* genus using GC-MS [110]. C₂₇H₄₄O was identified as 20-hydroxyecdysone, a sterol insect hormone, and synthesized by some plants as a defense mechanism from its invertebrate feeders [111, 112]. C₁₅H₂₂O₄ was identified as strobilactone, a fungal drimane sesquiterpene [113]. This molecular formula is also associated with leptospermone, a β -triketone found in *Leptospermum* and *Rhodomyrtus* plant genera, with α -glucosidase inhibitor activity [114]. LC-MS identified tentatively 4 cinchona alkaloids C₂₀H₂₆N₂O₂ and C₁₉H₂₂N₂O, common in *Cinchona* (Rubiaceae). In *Solanum* (Solanaceae), dasycarpidan-1-methanol, acetate (ester) was identified as a C₂₀H₂₆N₂O₂ isomer [115]. Another compound identified in *B. azurella* is azelaic acid; its glycoside has been proposed as a plant defense inducer in other Solanaceae species [116].

Table 6: identification of natural tentative top isomers by positive ionization LC-MS of BA.R.H₂O extract. Molecular formula (MF), abundance (related to the total signals), structural family, and associate bioactivity are shown.

MF	Abundance	Top Isomers(s)	Structural family	Bioactivity	Ref
C ₁₀ H ₈ O ₄	2.160	Scopoletin isomers	Hydroxycoumarin	Antioxidant, antimicrobial, anticancer, anti-inflammatory, and neuroprotector	[117]
C ₁₀ H ₈ O ₄	0.052				
C ₂₆ H ₄₂ O ₄	0.776	Hexadecyl ferulate	Coumaric acids and derivatives	Antioxidant	[118, 119]
C ₁₁ H ₁₆ O ₃	0.081	Loliolide isomers	Monoterpenoid	Neuroprotector, anti-inflammatory	[108, 109]
	0.072				
C ₂₇ H ₄₂ O ₄	0.055	Ruscogenin	Steroidal sapogenin	Inhibit cerebral, myocardial ischemic and acute kidney injury, anti-inflammatory, antioxidant, anticancer, gastric ulcer healing	[120–124]
C ₁₁ H ₁₀ O ₅	0.051	Fraxidin	Hydroxycoumarin	Anti-atopic effect, antibacterial and insulin mimetic activity	[125–127]
C ₂₇ H ₄₂ O	0.043	Cholest-4,6-Dien-3-One	steroid	Oxidation of cholesterol, induce cell proliferation, EMT markers, and senescence in hBTSC, impaired the differentiation in mature cholangiocytes.	[110, 128]
C ₂₇ H ₄₄ O ₇	0.039	20-Hydroxyecdysone	Sterol, hormone	Anabolic, hypolipidemic, antidiabetic, anti-inflammatory, hepato-neuro- and cardioprotector, antioxidant, antineoplastic	[111]
C ₂₇ H ₄₂ O ₃	0.038	Diosgenin	Steroidal sapogenin, triterpene	Diabetes, arthritis, osteoporosis, asthma, Alzheimer, cardiovascular, autoimmune and nervous system diseases. Antiviral, antineoplastic. Starting material for preparation of steroidal drugs.	[129]
C ₁₈ H ₃₀ O ₂	0.019	Linolenic acid	Fatty acid	Essential micronutrient. Antimetabolic syndrome, antithrombotic, anticancer, anti-inflammatory, antioxidant, neuroprotector	[130]

Table 7: identification of natural tentative top isomers by negative ionization LC-MS of BA.R.H₂O extract. Molecular formula (MF), abundance (related to the total signals), structural family, and associate bioactivity are shown.

MF	Abundance	Top Isomer(s)	Structural family	Bioactivity	Ref
C ₁₅ H ₂₂ O ₄	0.074	Strobilactone A	Drimane sesquiterpenoid	Marine-derived fungus. Antifungal activity	[113, 131]
C ₁₀ H ₈ O ₄	2.092	Scopoletin	Hydroxycoumarin	Antioxidant, antimicrobial, anticancer, anti-inflammatory, neuroprotector	[117]
C ₁₁ H ₁₀ O ₅	0.114	Isofraxidin	Hydroxycoumarin	Anticancer, antioxidant, cardioprotective, anti-inflammatory, neuroprotector	[132]
	0.099	Hydroquinidine isomers	Cinchona alkaloid	Anticarcinogenic, antiarrhythmic agent	[133, 134]
C ₂₀ H ₂₆ N ₂ O ₂	0.047				
	0.026				
C ₁₀ H ₁₀ O ₄	0.574	Ferulic acid	Phenol	Antioxidant, neuroprotector	[118]

C ₁₉ H ₂₂ N ₂ O	0.107	Cinchonine	Cinchona alkaloid	Antiparasitic, antimicrobial, anticancer, anti-obesity, anti-inflammatory, anti-platelet aggregation and anti-osteoclast differentiation	[135]
C ₉ H ₁₆ O ₄	0.068	Azelaic acid	Dicarboxylic acid	Anticancer, anti-comedolytic, antioxidant, anti-inflammatory, antimicrobial	[136]
C ₁₈ H ₃₂ O ₃	0.108	Dimorphecolic acid	Fatty acid	Highly reactive. Value for paints, inks, lubricants, plastic, and nylon manufacture	[137]
C ₇ H ₆ O ₂	0.077	3-Hydroxy benzaldehyde	Phenol	Vasculoprotector, antioxidant, wound healing. Angiostromylysis treatment.	[138]

4. CONCLUSION

This study represents the first comprehensive exploration of *B. azurella* from both chemical and biological perspectives. Although the specie does not exhibit significant antibacterial or anti-quorum sensing properties at tested concentrations, it does not exhibit acute toxicity and its anticancer effects warrant further investigation in this area. The root extract, rich in polyphenols, demonstrated notable antioxidant capacity and cytotoxic activity against colon cancer cells, indicating a positive correlation between these factors. Metabolomic analysis of the most active extract revealed the presence of biologically significant compounds such as coumarins, terpenes, steroidal saponinins, alkaloids and phenols. Future research will be able to take advantage of the results of this research by identifying active metabolites, or by exploring their effect on new cell lines.

ACKNOWLEDGEMENTS

The authors gratefully acknowledge the financial support of ANID Project “Strengthening of Doctoral Programs Call for Proposals 2022” (86220036), FONDEQUIP Project (EQM210006) and FONDEQUIP Project (EQM170172). D.D-H. express her gratitude to Magallanes University for the doctoral scholarship awarded and Málaga University for their help in conducting this research.

AUTHORS' CONTRIBUTIONS

Conceptualization: D.D-H, V.F Data curation: D.D-H Software: D.D-H Resources: V.F, R.A-D Formal Analysis: D.D-H, V.S, B.M-A, Investigation: D.D-H, Methodology: D.D-H, V.S, B.M-A, Supervision: V.F, R.A-D, J.B, Visualization: D.D-H Validation: D.D-H, V.F, R.A-D, J.B. Writing original draft: D.D-H Writing review & editing: D.D-H, V.F, R.A-D, J.B

REFERENCES

1. S. D. Matteucci, Ecorregión Estepa Patagónica, in Ecorregiones y Complejos Ecosistémicos Argentinos, Edited by J. Morello, S. D. Matteucci, A. F. Rodriguez, and M. Silva, Buenos Aires (2012), pp. 549–654.
2. C. Calfio and J. P. Huidobro-Toro, *Molecules* 24,2700 (2019).
3. L. Olivares-Caro, D. Nova-Baza, C. Radjokovic, L. Bustamante, D. Duran, D. Mennickent, V. Melin, D. Contreras, A. J. Perez, and C. Mardones, *Antioxidants* (Basel) 12, 304 (2023).
4. S. González, P. E. Guerra, H. Bottaro, S. Molares, M. S. Demo, M. M. Oliva, M. P. Zunino, and J. A. Zygadlo, *Flavour Fragr. J.* 19, 36 (2004).
5. M. Reina, O. Santana, D. M. Domínguez, L. Villarroel, V. Fajardo, M. L. Rodríguez, and A. González-Coloma, *Chem. Biodivers.* 9, 625 (2012).
6. C. Calderón-Reyes, R. S. Pezoa, P. Leal, A. Ribera-Fonseca, C. Cáceres, I. Riquelme, T. Zambrano, D. Peña, M. Alberdi, and M. Reyes-Díaz, *J. Soil Sci. Plant Nutr.* 20, 1891 (2020).
7. A. Soriano, *Darwiniana* 8,233 (1948).
8. S. Arroyo, *Bot. Not.* 133, 67 (1980).
9. M. V. Palchetti, J. J. Cantero, and G. E. Barboza, *An. Acad. Bras. Cienc.* 92 (2020).
10. E. Eich, *solanaceae and convolvulaceae: Secondary Metabolites*, Berlin, Germany, Springer Berlin, Heidelberg (2008).doi:10.1007/978-3-540-74541-9
11. M. Muñoz-Schick, A. Moreira-Muñoz, and S. MoreiraEspinoza, *Gayana Bot.* 69, 309 (2012).
12. R. Rodríguez, C. Marticorena, D. Alarcón, C. Baeza, L. Cavieres, V. L. Finot, N. Fuentes, A. Kiessling, M. Mihoc, A. Pauchard, E. Ruiz, P. Sanchez, and A. Marticorena, *Gayana Botánica* 75, 1 (2018).
13. A. M. Beeskow, M. A. Monsalve, and V. N. Duro, *An. del Instituto la Patagon.* 33, 5 (2005).
14. E. L. Sánchez-Montoya, M. A. Reyes, J. Pardo, J. Nuñez-Alarcón, J. G. Ortiz, J. C. Jorge, J. Bórquez, A. Mocan, and M. J. Simirgiotis, *Front. Pharmacol.* 8, 494 (2017).
15. G. Schmieda-hirschmann and C. Theoduloz, *J. Ethnopharmacol.* 228, 26 (2019).
16. R. R. Mosad, M. H. Ali, M. T. Ibrahim, H. M. Shaaban, M. Emara, and A. E. Wahba, *Phytochem. Lett.* 22, 167 (2017).
17. C. Mesas, M. Fuel, R. Martínez, J. Prados, C. Melguizo, and J. M. Porres, *Crit. Rev. Food Sci. Nutr.* 62, 6293 (2022).
18. G. Gong, Q. Liu, Y. Deng, T. Dang, W. Dai, T. Liu, Y. Liu, J. Sun, L. Wang, Y. Liu, T. Sun, S. Song, Z. Wang, and L. Huang, *Int. J. Biol. Macromol.* 149, 639 (2020).
19. M. Afroz, S. Akter, A. Ahmed, R. Rouf, J. A. Shilpi, E. Tiralongo, S. D. Sarker, U. Göransson, and S. J. Uddin, *Front. Pharmacol.* 11, 565 (2020).
20. A. Aisha, A. Arshad, S. Goher, and M. Iqbal, *Am. Int. J. Biol. Life Sci.* 2, 28 (2020).
21. C. Huanquilef, J. Espinoza, A. Mutis, L. Bardehle, E. Hormazabal, A. Urzúa, and A. Quiroz, *J. Soil Sci. Plant Nutr.* 21, 13 (2021).
22. C. Paz, V. Burgos, A. Iturra, R. Rebolledo, L. Ortiz, R. Baggio, J. Becerra, and C. L. Cespedes-acuña, *Ind. Crop. Prod.* 122, 232 (2018).
23. M. L. Parages, R. M. Rico, R. T. Abdala-Díaz, M. Chabrilón, T. G. Sotiroudis, and C. Jiménez, *J. Appl. Phycol.* 24, 1537 (2021).
24. H. H. Yeoh and Y. C. Wee, *Food Chem.* 49, 245 (1994).
25. M. Dubois, K. A. Gilles, J. K. Hamilton, P. A. Rebers, and F. Smith, *Anal. Chem.* 28, 350 (1956).
26. J. Folch, M. Lees, and G. H. Sloane Stanley, *J. Biol. Chem.* 226,497 (1957).
27. V. L. Singleton and J. A. Rossi, *Am. J. Enol. Vitic.* 16, 144 (1965).
28. W. Brand-Williams, M. E. Cuvelier, and C. Berset, *LWT - Food Sci. Technol.* 28, 25 (1995).
29. R. Re, N. Pellegrini, A. Proteggente, A. Pannala, M. Yang, and C. Rice-Evans, *Free Radic. Biol. Med.* 26, 1231 (1999).
30. R. T. Abdala Díaz, V. Casas Arrojo, M. A. Arrojo Agudo, C. Cárdenas, S. Dobretsov, and F. L. Figueroa, *Mar. Biotechnol.* 21, 577 (2019).
31. J. García-Márquez, A. Barany, Á. B. Ruiz, B. Costas, S. Arijio, and J. M. Mancera, *Fishes* 6, 61 (2021).
32. Y. M. Ibrahim, A. M. Abouwarda, and F. A. Omar, *Antonie VanLeeuwenhoek* 113, 1601 (2020).
33. P. Chen, N. U. Jung, V. Giarola, and D. Bartels, *Front. Plant Sci.* 10, 1698 (2019).
34. B. Plancot, B. Gügi, J. Mollet, C. Loutelier-Bourhis, S. R. Govind, P. Lerouge, M.-L. Follet-Gueye, M. Viceré, C. Alfonso, E. Nguema-ona, M. Bardor, and A. Driouich, *Carbohydr. Polym.* 208, 180 (2019).
35. A. San-Martín, M. Bacho, S. Nuñez, J. Roviroso, A. Soler, V. Blanc, R. León, and F. Olea, *J. Chil. Chem. Soc.* 63, 4082 (2018).
36. J. Bórquez, A. Ardiles, L. A. Loyola, L. M. Peña-Rodríguez, G. M. Molina-salinas, J. Vallejos, I. G. Collado, and M. J. Simirgiotis, *Molecules* 19,3898 (2014).
37. S. López, B. Lima, L. Aragón, L. A. Espinar, A. Tapia, S. Zacchino, J. Zygadlo, G. E. Feresin, and M. L. López, *Chem. Biodivers.* 9,1452 (2012).
38. J. H. Lee, D. Lee, J. J. Kang, H. T. Joo, J. H. Lee, H. W. Lee, S. H. Ahn, C. K. Kang, and S. H. Lee, *Biogeosciences* 14, 1903 (2017).
39. I. Trabelsi, S. Ben Slima, N. Ktari, M. Bouaziz, and R. Ben Salah, *Biomed Res. Int.* 6349019 (2021).doi:10.1155/2021/6349019
40. A. I. Ashurov, A. S. Dzhonmurodov, S. R. Usmanova, S. E. Kholov, and Z. K. Muhidinov, *Appl. Chem. Biotechnol.* 11, 281 (2021).
41. A. Rohman, R. Widyaningtyas, and F. Amalia, *Int. Food Res. J.* 24, 1362 (2017).
42. S. Mazurek, A. Mucciolo, B. M. Humbel, and C. Nawrath, *Plant J.* 74,880 (2013).
43. W. Qi, X. Zhou, J. Wang, K. Zhang, Y. Zhou, S. Chen, S. Nie, and M. Xie, *Carbohydr. Polym.* 237, 116113 (2020).
44. J. Zhang, C. Wen, H. Zhang, and Y. Duan, *Int. J. Biol. Macromol.* 139, 409 (2019).
45. Q. Guo, L. Ai, and S. Cui, *Methodology for Structural analysis of*

- polysaccharides, Springer Cham (2018).
46. D. Martinho and A. Karmali, *J. Can. Res. Updates* 8, 29 (2019).
 47. J. Liang, M. Zhao, S. Xie, D. Peng, M. An, Y. Chen, P. Li, and B. Du, *J. Food Biochem.* 46, e14355 (2022).
 48. B. Liao, D. Zhu, K. Thakur, L. Li, J. Zhang, and Z. Wei, *Molecules* 22, 2271 (2017).
 49. M. Zhang, N. Su, Q. Huang, Q. Zhang, Y. Wang, J. Li, and M. Ye, *J. Food Drug Anal.* 25, 976 (2017).
 50. K. Arunkumar, R. Raja, V. B. Sameer Kumar, A. Joseph, T. Shilpa, and I. S. Carvalho, *J. Food Meas. Charact.* 15, 567 (2021).
 51. R. Xu, X. Yang, J. Wang, H. Zhao, W. Lu, J. Cui, C.-L. Cheng, P. Zou, W.-W. Huang, P. Wang, W.-J. Li, and X.-L. Hu, *Int. J. Mol. Sci.* 13, 14262 (2012).
 52. S. M. Mäusle, N. Agarwala, V. G. Eichmann, H. Dau, D. J. Nürnberg, and G. Hastings, *Photosynth. Res.* 159, 229 (2024).
 53. S. Zaim, O. Cherkaoui, H. Rchid, R. Nmila, and R. El Moznie, *Polym. from Renew. Resour.* 11, 49 (2020).
 54. J. Vega, T. S. Catalá, J. García-Márquez, L. G. Speidel, S. Arijó, N. Cornelius Kunz, C. Geisler, and F. L. Figueroa, *Mar. Drugs* 21, 5 (2022).
 55. P. Chandran R, *MOJ Food Process. Technol.* 4, 74 (2017).
 56. M. Mandal, D. Misra, N. N. Ghosh, and V. Mandal, *Asian Pac. J. Trop. Biomed.* 7, 979 (2017).
 57. M. Arif, Y. Li, M. M. El-Dalatony, C. Zhang, X. Li, and E.-S. Salama, *Renew. Energy* 163, 1973 (2021).
 58. S. Radic-Schilling, P. Corti, R. Muñoz-Arriagada, N. Butorovic, and L. Sánchez-Jardón, *Capítulo 7. Ecosistemas de estepa en la Patagonia chilena: distribución, clima, biodiversidad y amenazas para su manejo sostenible, in Conservación en la Patagonia chilena: evaluación del conocimiento, oportunidades y desafíos*, Edited by M. J. Castilla, J. C., Arnesto, J. J., Martínez-Harms, Santiago, Chile, Ediciones Universidad Católica (2021), pp. 223–256.
 59. I. Hameed and F. Hussain, *Pak. J. Pharm. Sci.* 28, 1203 (2015).
 60. E. Reszczy and A. Hanaka, *Cell Biochem. Biophys.* 78, 401 (2020).
 61. V. Lokapur, V. Jayakar, and M. Shantaram, *Biomedicine* 40, 460 (2020).
 62. M. de Armas-Ricard, F. Quinán-Cardenas, H. Sanhueza, R. Pérez-Vidal, C. Mayorga-lobos, and O. Ramírez-Rodríguez, *Molecules* 26, 6722 (2021).
 63. S. Singh, M. F. Sk, A. Sonawane, P. Kar, and S. Sadhukhan, *J. Biomol. Struct. Dyn.* 39, 6249 (2021).
 64. I. Gülçin, A. C. Gören, P. Taslimi, S. H. Alwasel, O. Kilic, and E. Bursal, *Biocatal. Agric. Biotechnol.* 23, 101441 (2020).
 65. I. Dominguez-lópez, M. Pérez, and R. M. Lamuela-Raventós, *Crit. Rev. Food Sci. Nutr.* 1 (2023). doi:10.1080/10408398.2023.2220031
 66. J. Vega, F. Álvarez-Gómez, L. Güenaga, F. L. Figueroa, and J. L. Gómez-Pinchetti, *Aquaculture* 522, 735088 (2020).
 67. R. Bridi, M. J. Troncoso, C. Folch-Cano, J. Fuentes, H. Speisky, and C. López-Alarcón, *Food Anal. Methods* 7, 2075 (2014).
 68. X. Hu, D. Dong, M. Xiab, Y. Yanga, J. Wanga, J. Sua, L. Sun, and H. Yu, *New J. Chem.* 44, 11405 (2020).
 69. Y. A. Hajam, R. Rani, S. Y. Ganie, T. A. Sheikh, D. Javaid, S. S. Qadri, S. Pramodh, A. Alsulimani, M. F. Alkhanani, S. Harakeh, A. Hussain, S. Haque, and M. S. Reshi, *Cells* 11, 552 (2022).
 70. S. Anwar, M. Faisal Nadeem, I. Pervaiz, U. Khurshid, N. Akmal, K. Aamir, M. Haseeb ur Rehman, K. Almansour, F. Alshammari, M. F. Shaikh, M. Locatelli, N. Ahemad, and H. Saleem, *Front. Plant Sci.* 13, 988352 (2022).
 71. H. F. Zohra, E. Ramazan, and H. Ahmed, *Acta Biológica Colomb.* 27, 403 (2021).
 72. K. Ghafoor, F. Al Juhaimi, M. M. Özcan, N. Uslu, E. E. Babiker, and I. A. Mohamed Ahmed, *LWT - Food Sci. Technol.* 126, 109354 (2020).
 73. A. Saffaryazdi, A. Ganjeali, R. Farhoosh, and M. Cheniany, *Physiol. Mol. Biol. Plants* 26, 1519 (2020).
 74. N. Nagahama, B. Gastaldi, M. N. Clifford, M. M. Manifesto, and R. H. Fortunato, *AIMS Agric. Food* 6, 106 (2020).
 75. R. Wolosiak, B. Dru, D. Derewiaka, M. Piecyk, E. Majewska, M. Ciecierska, E. Worobiej, and P. Pakosz, *Molecules* 27, 50 (2022).
 76. B. Gastaldi, Y. Assef, C. Van Baren, P. Di Leo Lira, D. Retta, A. L. Bandoni, and S. B. González, *Rev. Cuba. Plantas Med.* 21, 51 (2016).
 77. M. Karama'c, F. Gai, E. Longato, G. Meineri, M. A. Janiak, R. Amarowicz, and P. G. Peiretti, *Antioxidants* 8, 173 (2019).
 78. F. Jiménez-Aspee, S. Thomas-Valdés, A. Schulz, A. Ladio, C. Theoduloz, and G. Schmieda-Hirschmann, *Food Sci. Nutr.* 4, 595 (2015).
 79. M. C. Varela, I. Arslan, M. A. Reginato, A. M. Cenzano, and M. V. Luna, *Plant Physiol. Biochem.* 104, 81 (2016).
 80. M. R. Islam, S. Ahmed, S. I. Sadia, A. K. Sarkar, and M. A. Alam, *Asian J. Res. Biochem.* 13, 43 (2023).
 81. O. P. N. Yarley, A. B. Kojo, C. Zhou, X. Yu, A. Gideon, H. H. Kwadwo, 117. L. D. Antika, A. N. Tasfiyati, H. Hikmat, and A. W. Septama, *Zeitschrift* and O. Richard, *Int. J. Biol. Macromol.* 183, 2262 (2021).
 82. J. M. Calderón-Montaño, S. M. Martínez-Sánchez, V. Jiménez-González, E. Burgos-Morón, E. Guillén-Mancina, J. J. Jiménez-Alonso, P. Díaz-Ortega, F. García, A. Aparicio, and M. López-Lázaro, *Plants (Basel)* 10, 2193 (2021).
 83. B. Gastaldi, G. Marino, Y. Assef, F. M. Silva Sofrás, C. A. N. Catalán, and S. B. González, *Plant Foods Hum. Nutr.* 73, 180 (2018).
 84. P. Rohilla, H. Jain, A. Chhikara, L. Singh, and P. Dahiya, *South African J. Bot.* 149, 269 (2022).
 85. W. Ahmed, D. Mofed, A. Zekri, N. El-sayed, M. Rahouma, and S. Sabet, *J. Int. Med. Res.* 46, 1358 (2018).
 86. D. H. Abou Baker and H. M. Rady, *Plant Arch.* 20, 3285 (2020).
 87. D. O. Nkwe, B. Lotshwao, G. Rantong, J. Matshwele, T. E. Kwape, K. Masisi, G. Gaobotse, K. Hefferon, and A. Makhzoum, *Cancers (Basel)* 13, 4989 (2021).
 88. N. Fadl Almoulah, Y. Vovnikov, R. Gevrenova, H. Schohn, T. Tzanova, S. Yagi, J. Thomas, B. Mignard, A. A. A. Ahmed, M. A. El Siddig, R. Spina, and D. Laurain-mattar, *South African J. Bot.* 112, 368 (2017).
 89. F. S. Mohammed, E. Kina, M. Sevindik, M. Dogan, and M. Pehlivan, *Turkish J. Agric. - Food Sci. Technol.* 9, 818 (2021).
 90. L. Manosalva, A. Mutis, A. Urzúa, V. Fajardo, and A. Quiroz, *Molecules* 21, 76 (2016).
 91. I. Montenegro, M. Valenzuela, N. Zamorano, R. Santander, C. Baez, and A. Madrid, *Nat. Prod. Res.* 35, 2072 (2021).
 92. N. B. Turan and G. Ö. Engin, *Quorum Quenching, in Fundamentals of Quorum Sensing, Analytical Methods and Applications in Membrane Bioreactors, Comprehensive Analytical Chemistry* (2018), pp. 117–149.
 93. X. Zhao, Z. Yu, and T. Ding, *Microorganisms* 8, 425 (2020).
 94. G. Singh, E. Tamboli, A. Acharya, C. Kumarasamy, K. Mala, and P. Raman, *Med. Hypotheses* 84, 539 (2015).
 95. F. Moradi and N. Hadi, *New Microbes New Infect.* 42, 100882 (2021).
 96. P. Kusari, S. Kusari, M. Lamshöft, S. Sezgin, M. Spiteller, and O. Kayser, *Appl. Microbiol. Biotechnol.* 98, 7173 (2014).
 97. B. X. ValenciaQuecán, M. L. Castillo Rivera, and U. M. Pinto, Chapter 19. Bioactive phytochemicals targeting microbial activities mediated by quorum sensing, *Springer Nature Singapore Pte Ltd.* (2018). doi:10.1007/978-981-10-9026-4_19
 98. X. Yi, Z. Gao, L. Liu, Q. Zhu, G. Hu, and X. Zhou, *Front. Environ. Sci. Eng.* 14, 109 (2020).
 99. S. Parvez, C. Venkataraman, and S. Mukherji, *Environ. Int.* 32, 265 (2006).
 100. E. C. Faria, B. J. Treves Brown, and R. D. Snook, *J. Environ. Monit.* 6, 97 (2004).
 101. M. D. Hernando, S. De Vettori, M. J. Martínez Bueno, and A. R. Fernández-Alba, *Chemosphere* 68, 724 (2007).
 102. M. K. Patel, S. Pandey, M. Kumar, M. I. Haque, S. Pal, and N. S. Yadav, *Plants* 10, 2409 (2021).
 103. F. Domergue and D. K. Kosma, *Plants* 6, 25 (2017).
 104. K. Poralla, Cycloartenol and other triterpene cyclases, in "Comprehensive Natural Products Chemistry" Vol. 2, Edited by Sir Derek Barton and Koji Nakanishi, Pergamon Press, Elsevier (1999), pp. 299–319.
 105. N. Nasr, M. Elbatany, and M. A. Hamed, *Chem. Biodivers.* e202401102 (2024). doi:10.1002/cbdv.202401102
 106. S. C. Chou, T. J. Huang, E. H. Lin, C. H. Huang, and C. H. Chou, *Nat. Prod. Commun.* 7, 153 (2012).
 107. M. Murata, Y. Nakai, K. Kawazu, M. Ishizaka, H. Kajiwara, H. Ab, K. Takeuchi, Y. Ichinose, I. Mitsuhashi, A. Mochizuki, and S. Seo, *Plant Physiol.* 179, 1822 (2019).
 108. T. U. Jayawardena, H. Kim, K. K. A. Sanjeewa, S. Kim, J.-R. Rho, Y. Jee, G. Ahn, and Y. Jeon, *Algal Res.* 40, 101513 (2019).
 109. J. Silva, C. Alves, A. Martins, P. Susano, M. Simões, M. Guedes, S. Rehfeldt, S. Pinteus, H. Gaspar, A. Rodrigues, M. I. Goettert, A. Alfonso, and R. Pedrosa, *Int. J. Mol. Sci.* 22, 1888 (2021).
 110. M. A. Asiamah, T. A. Agana, Y. D. Boakye, C. Agyare, and F. Adu, *J. Parasitol. Res.* 2024, 5513489 (2024).
 111. O. Shuvalov, Y. Kirdeeva, E. Fefilova, S. Netsvetay, M. Zorin, Y. Vlasova, O. Fedorova, A. Daks, S. Parfenyev, and N. Barlev, *Metabolites* 13, 656 (2023).
 112. A. Suksamrarn, S. Kumpun, and B.-E. Yingyongnarongkul, *J. Nat. Prod.* 65, 1690 (2002).
 113. Y. Huang and V. Valiante, *ChemBioChem* 23, e202200173 (2022).
 114. D. Ferlinahayati, E. Alfaredo, and B. Untari, *Indones. J. Chem.* 20, 307 (2020).
 115. J. K. P. Y. Sundar S., *Asian J. Pharm. Clin. Res.* 8, 179 (2015).
 116. M. I. Mhlongo, L. A. Pieter, P. A. Steenkamp, N. Labuschagne, and I. A. Dubery, *Metabolites* 16, 466 (2022).
 - fur Naturforsch. - Sect. C J. Biosci. 77, 303 (2022).

118. J. Nadal, F. de B. Pedroso, B. R. Minozzo, P. Salles de Brito, P. V. Farago, J. C. R. Velloso, and E. Miyoshi, *Brazilian Arch. Biol. Technol.* 61 (2018).
119. C. Singh, R. K. Saxena, and P. Tripathi, *Int. J. Pharm. Qual. Assur.* 14, 119 (2023).
120. Z. Song, X. Xiang, J. Li, J. Deng, Z. Fang, L. Zhang, and J. Xiong, *Oncol. Rep.* 43, 516 (2020).
121. G. Cao, N. Jiang, Y. Hu, Y. Zhang, G. Wang, M. Yin, X. Ma, K. Zhou, J. Qi, B. Yu, and J. Kou, *Int. J. Mol. Sci.* 17, 1418 (2016).
122. G. Ercan, R. Ilbar Tartar, A. Solmaz, O. B. Gulcicek, O. O. Karagulle, S. Meric, H. Cayoren, R. Kusaslan, A. Kemik, D. Gokceoglu Kayali, S. Cetinel, and A. Celik, *Asian J. Surg.* 43, 405 (2020).
123. F. Fu, Q. Lai, J. Hu, L. Zhang, X. Zhu, J. Kou, B. Yu, and F. Li, *Antioxidants (Basel)* 11, 583 (2022).
124. M. Hu and S. An, *Comput. Intell. Neurosci.* 2022, 8066126 (2022).
125. T. Y. Kim, B. Jo, N. Park, Y. Park, S. Kim, and M. H. Yang, *Nat. Prod. Sci.* 27, 251 (2021).
126. J. Lee, D. Jung, W. Kim, J. Um, S. Yim, W. K. Oh, and D. R. Williams, *ACS Chem. Biol.* 8, 1803 (2013).
127. N. A. Mfonku, A. T. Tadjong, G. T. Kamsu, N. Kodjio, J. Ren, J. A. Mbah, D. Gatsing, and J. Zhan, *Chem. Pap.* 75, 2067 (2021).
128. L. Nevi, D. Costantini, S. Safarikia, S. Di Matteo, F. Melandro, P. B. Berloco, and V. Cardinale, *Cells* 8, 1443 (2019).
129. P. Semwal, S. Painuli, T. Abu-izneid, A. Rauf, A. Sharma, S. D. Daştan, M. Kumar, M. M. Alshehri, Y. Taheri, R. Das, S. Mitra, T. Bin Emran, J. Sharifi-Rad, D. Calina, and W. C. Cho, *Oxid. Med. Cell. Longev.* 2022, 1035441 (2022).
130. Q. Yuan, F. Xie, W. Huang, M. Hu, Q. Yan, Z. Chen, Y. Zheng, and L. Liu, *Phyther. Res.* 36, 164 (2022).
131. E. Cohen, L. Koch, K. M. Thu, Y. Rahamim, Y. Aluma, M. Ilan, O. Yarden, and S. Carmeli, *Bioorg. Med. Chem.* 19, 6587 (2011).
132. M. B. Majnooni, S. Fakhri, Y. Shokoohinia, M. Mojarab, S. Kazemi-Afrakoti, and M. H. Farzaei, *Molecules* 25, 2040 (2020).
133. M. Yavuz and T. Demircan, *Mol. Biol. Rep.* 50, 2611 (2023).
134. R. Pemmereddy, K. S. Chandrashekar, S. R. K. Pai, V. Pai, A. Mathew, and B. Venkatesh Kamath, *Rasayan J. Chem.* 15, 1 (2022).
135. S. Parveen, N. Maurya, A. Meena, and S. Luqman, *Curr. Top. Med. Chem.* 24, 343 (2024).
136. A. Kumar, R. Rao, and P. Yadav, *Curr. Drug ther.* 15, 181 (2022).
137. J. M. S. Faria, *Biol. Life Sci. Forum* 27, 4 (2023).
138. K.-Y. Chen, Y.-J. Chen, C.-J. Cheng, K.-Y. Jhan, C.-H. Chiu, and L.-C. Wang, *Biomed. J.* 44, S258 (2021).